Eur Phys J C **41**, s02, 1–10 (2005)
Digital Object Identifier (DOI) 10.1140/epjcd/s2005-02-006-0

EPJ C direct
electronic only

Scientific Note

Production of excited neutrinos at the LHC

A. Belyaev[1], C. Leroy[2], R. Mehdiyev[2,3]

[1] Department of Physics, Florida State University, Tallahassee, FL, USA
[2] Université de Montréal, Département de Physique, Montréal, H3C 3J7, Canada
[3] on leave of absence from Institute of Physics, Azerbaijan National Academy of Sciences, 370143, Baku, Azerbaijan

Received: 24 January 2005 / Revised version: 7 April 2005 /
Published online: 28 April 2005 –

Abstract. We study the potential of the CERN LHC to observe excited neutrinos resulting from the single production process through gauge interactions and decaying in various channels. The mass range accessible with the ATLAS detector is determined.

PACS. 12.60.Rc, 13.85.Rm

1 Introduction

The proliferation of quarks and leptons can be naturally explained by the assumption that they are composite objects. According to models of compositeness [1], known fermions are bound states of more fundamental constituents – preons [2] or a fermion and a boson [3]. In the framework of these models, constituents of known fermions interact by means of new strong gauge interactions.

One of the main consequences of the non-trivial substructure of the standard model (SM) fermions would be a rich spectrum of excited states [1,4]. Observation of such fermionic excitations would be clear evidence of the underlying substructure of known fermions. Therefore, one of the tasks of great importance for TeV energy scale colliders is to probe the possible substructure of leptons and quarks and test the predictions of composite models.

The SM can be considered as the low energy limit of a more fundamental theory which is characterized by a large mass scale Λ. The existence of four-fermion contact interactions would be a signal of new physics beyond the SM. The nature of this new physics can be probed if the experimental energy scale is high enough. It is expected that the next generation of hadron colliders, like the LHC, will achieve very high centre of mass energies. Experiments at the LHC will thus extend the search for composite states. In particular, contact interactions may be an important source for excited lepton production.

The excited states of the SM fermions can interact via SM gauge field interactions and also via new gauge strong interactions between preons. The latter leads to effective contact interactions between quarks and leptons and/or their excited states in the low energy limit.

Contact interactions could become manifest as an excess in Drell-Yan dilepton production at the LHC, even for very large values of the compositeness scale. The sensitivity of the LHC is very high: up to $\Lambda = 30$ TeV for an integrated luminosity of 100 fb^{-1} [5]. If the compositeness scale is higher than the excited neutrino mass, then direct production of the excited states of fermions will proceed by gauge interactions, as contact interactions will be significantly suppressed. This is the subject of the present paper, where we study direct production of the excited neutrinos by gauge interactions at the LHC.

Many recent experimental studies have been devoted to the search for quark and lepton compositeness and excited states at LEP [6], HERA [7], and the Tevatron [8]. No evidence of excited fermions has been found so far. The studies mentioned above put limits: i) on the compositeness scale in the range of 2-8 TeV, depending on the type of the contact interactions, and ii) on the excited fermion mass up to the collider center-of-mass energy. The current lower bound of the excited neutrino mass, obtained from the $e^+e^- \to \nu^\star\nu^\star$ process, is 102.6 GeV. This limit assumes a dominant $\nu^\star \to \nu\gamma$ decay mode. The limit for excited $\nu^\star$ mass, from single production $e^+e^- \to \nu\nu^\star$, is 190 GeV and depends on the transition magnetic coupling between ν/e and $\nu^\star$. Both of these mass limits were obtained at LEP [6].

Based on previous studies [4]-[12], we expect that the LHC collider will put stringent constraints on composite models and/or the masses of excited fermions.

The aim of this article is to evaluate the ultimate potential of the LHC collider for discovery of excited neutrinos, which has not been studied in detail, previously. The work is a continuation of earlier studies devoted to excited quark and excited electron production [10].

The article is organized as follows. In Sect. 2, we discuss effective Lagrangians for models used for our study. Section 3 presents details of our study and results. Section 4 shows the mass reach, while Sect. 5 outlines the conclusions.

2 Physical setup

For the sake of simplicity we limit the number of parameters in our study and assume the simplest realization of the model, where the excited fermions are isospin $\frac{1}{2}$ partners and their spin is $\frac{1}{2}$ (higher spin representations are considered in [13], for example).

We also assume that an excited fermion has acquired mass before SU(2)⊗U(1) symmetry breaking has taken effect. Therefore, we consider their left- and their right-components in isodoublets. For example, we have the following assignments for the first generation of fermions:

$$l_L = \begin{pmatrix} \nu_e \\ \mathrm{e} \end{pmatrix}_L , \; e_R ,$$
$$l_L^\star = \begin{pmatrix} \nu_e^\star \\ \mathrm{e}^\star \end{pmatrix}_L , \quad l_R^\star = \begin{pmatrix} \nu_e^\star \\ \mathrm{e}^\star \end{pmatrix}_R$$
$$q_L = \begin{pmatrix} \mathrm{u} \\ \mathrm{d} \end{pmatrix}_L ; \quad q_R = \mathrm{u}_R, \mathrm{d}_R ;$$
$$q_L^\star = \begin{pmatrix} \mathrm{u}^\star \\ \mathrm{d}^\star \end{pmatrix}_L ; \quad q_R^\star = \begin{pmatrix} \mathrm{u}^\star \\ \mathrm{d}^\star \end{pmatrix}_R ;$$

In order to avoid conflict with precision measurements of the anomalous magnetic moment of muons (g-2) and to protect light fermions from large radiative corrections, one should require a chiral form of interactions of excited fermions with SM ones [14].

The couplings of excited fermions ($f^\star = l^\star, q^\star$) to gauge bosons are vector like:

$$L_{\mathrm{eff}}^{\mathrm{1gauge}} = \bar{f}^\star \gamma^\mu \left(f_s g_s \frac{\boldsymbol{\lambda^a}}{2} \boldsymbol{G^a}_\mu + f g \frac{\boldsymbol{\tau}}{2} \boldsymbol{W}_\mu + f^{'} g^{'} \frac{Y}{2} B_\mu \right) f^\star, \quad (1)$$

while transitions between ordinary and excited fermions are uniquely fixed by magnetic-moment type gauge-invariant interactions [15]:

$$L_{\mathrm{eff}}^{\mathrm{2gauge}} = \frac{1}{2\Lambda} \bar{f}_{\mathrm{R}}^\star \sigma^{\mu\nu} \left(f_s g_s \frac{\boldsymbol{\lambda^a}}{2} \boldsymbol{G^a}_{\mu\nu} + f g \frac{\boldsymbol{\tau}}{2} \boldsymbol{W}_{\mu\nu} + f^{'} g^{'} \frac{Y}{2} B_{\mu\nu} \right) f_{\mathrm{L}} + \mathrm{h.c.}, \quad (2)$$

where Λ is the compositeness scale. $\boldsymbol{G^a}_{\mu\nu}$, $\boldsymbol{W}_{\mu\nu}$ and $B_{\mu\nu}$ are SU(3), SU(2) and U(1) tensors with the coupling constants g_s, g and $g^{'}$, respectively; Y is the weak hypercharge with Y = (-1) and (1/3) for leptons and quarks, respectively; f_s, f and f' are parameters depending on the underlying dynamics.

The Lagrangian in definition 2 gives rise to the following $fermion - fermion^\star - gauge\ boson$ vertices:

$$\Gamma_\mu^{g\bar{f}^\star f} = \frac{g_s f_s}{2\Lambda} q^\nu \sigma_{\mu\nu} (1 - \gamma^5) \quad (3)$$
$$\Gamma_\mu^{\gamma\bar{f}^\star f} = \frac{e}{2\Lambda} [e_f f' + I_3 (f - f')] q^\nu \sigma_{\mu\nu} (1 - \gamma^5) \quad (4)$$
$$\Gamma_\mu^{Z\bar{f}^\star f} = \frac{e}{2\Lambda} \frac{I_3 (c_W^2 f + s_W^2 f') - 4 e_f s_W^2 f'}{s_W c_W} \times q^\nu \sigma_{\mu\nu} (1 - \gamma^5) \quad (5)$$
$$\Gamma_\mu^{W\bar{f}^\star f} = \frac{e}{2\Lambda} \frac{f}{\sqrt{2} s_W} q^\nu \sigma_{\mu\nu} (1 - \gamma^5), \quad (6)$$

where I_3 is the weak isospin of the excited fermion, e_f is its charge in units of the proton charge, $s_W (c_W)$ is the sine(cosine) of the weak mixing angle.

Excited fermions can be produced in pairs via interactions given by Eq. (1) as well as singly via interactions given by Eq. (2). In this article, we study the production of single excited neutrinos of the first generation. The single production of excited neutrinos is less kinematically suppressed than the production of a pair of excited neutrinos. Therefore, when the $\nu - \nu^\star - V$ coupling is not significantly suppressed by the compositeness scale Λ (one should recall that this coupling is proportional to the momenta of the photon which partially compensates the Λ suppression) compared to the coupling $\nu^\star - \nu^\star - V$, the process of the single excited neutrino production is better suited for establishing the limits on the excited neutrino mass.

Excited neutrinos can be singly produced at the LHC via the neutral current process (see Fig. 1):

$$q\bar{q} \to \nu\nu^\star, \quad (7)$$

or via a charged current, in association with an electron (see Fig. 2)

$$q\bar{q'} \to e\nu^\star. \quad (8)$$

One should notice that excited neutrinos can be also produced via contact interactions resulting from preon interactions. This scenario for the case of excited electron production has been studied previously [12].

In general, the couplings f and f' involved in single excited neutrino production are not equal to each other.

Fig. 1. Diagrams for single excited neutrino ($\nu^\star$) production via Z-boson and photon exchange

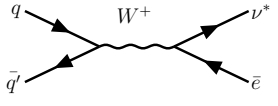

Fig. 2. Diagram for single excited neutrino ($\nu^\star$) production via W-boson exchange

Table 1. Cross sections (CompHEP) (in fb) for $q\bar{q} \to \nu^\star l$ and scale $\Lambda = m^\star$

$m^\star$(GeV)		500	1000	1500	2000	2500
pp $\to e\nu^\star$		121.	5.99	7.43×10^{-1}	1.32×10^{-1}	2.82×10^{-2}
pp $\to \nu\nu^\star$	$f = f' = 1$	65.3	3.07	3.67×10^{-1}	6.40×10^{-2}	1.36×10^{-2}
	$f = -f' = 1$	70.5	3.37	4.09×10^{-1}	7.21×10^{-2}	1.55×10^{-2}

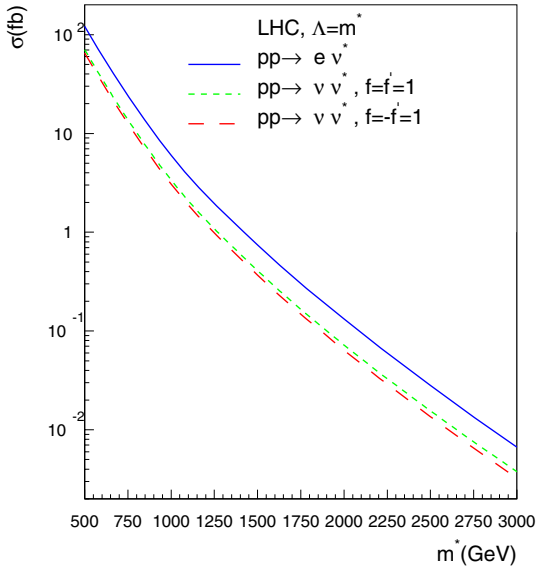

Fig. 3. Cross section for single excited neutrino production versus the excited neutrino mass, $m^\star$ at LHC for $\Lambda = m^\star$. Dashed and dotted lines denote $f = f' = 1$ and $f = -f' = 1$ choices, respectively, for the case of excited neutrino production via neutral currents. The cross sections shown account for the production of both excited neutrino and excited antineutrino at LHC

Therefore, the $\gamma\nu\nu^\star$ coupling which is proportional to $(f - f')$ can be non-vanishing. In Fig. 3, we present the cross sections for the processes (7) and (8) as a function of the excited neutrino mass, $m^\star$ ($\Lambda = m^\star$) for two cases studied in this article: $f = f' = 1$ and $f = -f' = 1$. The corresponding values for the cross sections are presented in Table 1. The choice of $\Lambda = m^\star$ is used here as a convenient reference value, and the constraints which will be obtained on f/Λ can be trivially rescaled. The cross section values were calculated using the CTEQ5L parton distribution function (PDF) [16]. The QCD scale has been chosen equal to the excited neutrino mass. We have checked that the systematic uncertainty due to the choice of others PDF sets is about 20%.

Excited neutrinos will decay to $\nu\gamma$, νZ and eW, giving rise to $\nu\nu\gamma$, $\nu\nu\nu$, νll, νqq, $e\nu l$ and eqq particles in the final state. Branching ratios for excited neutrino decays, which are defined by gauge interactions and f and f' couplings, are presented in Table 2 for the two cases considered. One can see that for the case $f = -f' = 1$, where the $\gamma\nu\nu^\star$ couplings do not vanish, the branching ratio $Br(\nu^\star \to \gamma\nu)$ is of the order of 30%. In this case, the role of the $\nu\gamma$ channel would be significant. For excited neutrino masses

Table 2. Branching ratios (in %) of excited neutrino decay via gauge interactions

process		for $m^\star$(GeV)	
		500	> 1000
$f = f' = 1$	$\nu^\star \to We$	61	61
	$\nu^\star \to Z\nu$	39	39
	$\nu^\star \to \gamma\nu$	0	0
$f = -f' = 1$	$\nu^\star \to We$	60	61
	$\nu^\star \to Z\nu$	12	12
	$\nu^\star \to \gamma\nu$	28	27

$m^\star > 500$ GeV, much greater than M_Z, M_W, branching ratios of the excited neutrino decay do not depend on the mass (see Table 2).

3 Simulations and results

Simulations of excited lepton signals and relevant backgrounds were performed with the chain of programs CompHep [17], the CompHep-PYTHIA interface [18] and PYTHIA [19]. The ATLFAST [20] code was used to take into account the experimental conditions prevailing at the LHC for the ATLAS detector. The detector concept and its physics potential have been presented in the ATLAS Technical Proposal [21] and the ATLAS Technical Design Report [5]. The ATLFAST program for fast detector simulations accounts for most of the detector features: jet reconstruction in the calorimeters, momentum/energy smearing for leptons and photons, magnetic field effects and missing transverse energy. It provides a list of reconstructed jets, isolated leptons and photons. In most cases, the detector dependent parameters were tuned to values expected for the performance of the ATLAS detector obtained from full simulation.

The electromagnetic calorimeters were used to reconstruct the energy of leptons in cells of dimensions $\Delta\eta \times \Delta\phi = 0.025 \times 0.025$, where ϕ is the azimuthal angle and η is the pseudorapidity, within the pseudorapidity range $-2.5 < \eta < 2.5$. The electromagnetic energy resolution is given by $0.1/\sqrt{E(GeV)} \bigoplus 0.007$ over this pseudorapidity region. iThe electromagnetic showers are identified as electrons when they lie within a cone of radius $\Delta R = \sqrt{(\Delta\eta)^2 \times (\Delta\phi)^2} = 0.2$ and when they possess a transverse energy $E_T > 5$ GeV. Electron isolation criteria were applied, requiring a distance $\Delta R > 0.4$ from other clusters and maximum transverse energy deposition,

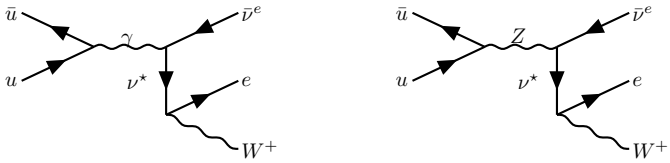

Fig. 4. Diagram for the production of an excited neutrino ($\nu^\star$) in association with an anti-neutrino, where $\nu^\star$ decays to W and electron (e)

$E_T < 10$ GeV, in cells in a cone of radius $\Delta R = 0.2$ around the direction of lepton emission.

It must be mentioned that standard parameterizations in the ATLFAST Monte Carlo program have been chosen for the leptonic resolution but detailed studies are needed, using test beam data and GEANT full simulation to validate the extrapolation of the resolution function to leptonic energies in the TeV range. This study is mainly restricted to the use of the calorimetric systems of ATLAS. However, the use of ATLAS inner detector information would only improve our sensitivity. ATLFAST does not take into account efficiencies for identifying electron and/or misidentifying jet. We apply a 90% identification efficiency for electrons, photons and muons which should be reachable in ATLAS at the high LHC luminosity [5] [1].

The presence of pile-up events, should not be problem in our case due to a very high transverse momentum of the excited neutrino decay products. We are planning to address the question of a pile-up in the context of a study of fully simulated excited neutrino production events in near future.

3.1 Neutral current process $q\overline{q} \to \nu^\star\nu$

For this type of subprocess, we consider only the decay of excited neutrinos to a W and an electron mediated by gauge interactions. We assume here that the generation mixing is absent and the excited neutrino is lighter than the $e^\star$, so the $\nu^\star \to We^\star$ decay chain is kinematically forbidden. Typical Feynman diagrams relevant for the $\nu^\star \to We$ process are shown in Fig. 4. For the W decay, we limit ourselves to the case $W \to$ jets since, in the case of semileptonic decays of W, the final state consists of two neutrinos, giving a large uncertainty in the excited neutrino mass reconstruction. The signal signature for the selected reaction ($\nu^\star \to We$) consists of an electron, two jets and missing transverse energy.

We considered three SM backgrounds:

- $t\bar{t}$ pair production, where top quarks always decay to Wb, and where one W decays to jets and the second W decays into an electron and a neutrino.
- $q\overline{q} \to WW$ pair production with the same decays as above.
- W + jets production, where the W decays to an electron and a neutrino.

[1] to confirm these numbers some additional studies might be needed.

The single top production in the $gb \to tW$ process contributes at the level of 20-30% to $t\bar{t}$ background. Since the contribution of $t\bar{t}$ events to the overall background is not significant for the subprocesses and cuts we have studied (shown below), we have not presented this background in this article.

The following cuts were used to separate the signal from background:

- The transverse momentum of the electron was required to be at least 150 (250, 300) GeV for $m^\star$ masses of 500, (750, 1000) GeV, respectively, and to be emitted in the pseudorapidity region $\eta < 2.5$.
- The transverse momenta of two jets were required to be at least 50 GeV.
- The mass of the W reconstructed from any two jets was required to be in the mass window $60 - 100$ GeV (mainly to suppress the dominant $W(\to e\nu)$+jets background).
- The missing transverse momentum, $\not{P}_T$, was required to be at least 250, (350, 350) GeV for $m^\star$ masses of 500, (750, 1000) GeV, respectively.

The resulting invariant mass distributions of the (electron-jet-jet) system are presented in Fig. 5 for the mass of the excited neutrino $m^\star = 500$ GeV (left) and $m^\star = 1000$ GeV (right). The resonances are clearly seen above the total background. The $W+$ jets is a dominant background for this case. The distributions were normalized to an integrated luminosity of $L = 300$ fb^{-1}.

3.2 Charged current processes $q\overline{q} \to e\nu^\star$

3.2.1 Channel with $\nu^\star \to We$ decay.

Here again we considered the decay of excited neutrinos to We, mediated by gauge interactions (Fig. 6). For W decays we took into consideration several options.

W decay to $e\nu$. In this case the final state consists of three electrons and a neutrino. The signal signature is sought in the system of two electrons and a neutrino. For this final state we studied two SM backgrounds:

- $W + Z$ production, where W decays into $e\nu$ and Z decays into an electron - positron pair. Events were produced with PYTHIA and CTEQ5L for partonic transverse momentum $\hat{p}_T > 200$ GeV with the corresponding cross section, $\sigma \times BR = 1.23 fb$.
- WWW production, where each W decays into an electron and a neutrino. This type of background events has been produced with CompHep with the total cross section of 0.14 pb.

We considered all possible combinations of ($ee\nu$) as a candidate for $\nu^\star$, taking into account that only leptons with opposite charge should contribute to this signature.

The following cuts were used to separate the signal from background:

- The transverse momentum of each of the three electrons was required to be at least 50 GeV and to be within the pseudorapidity acceptance of $\eta < 2.5$.

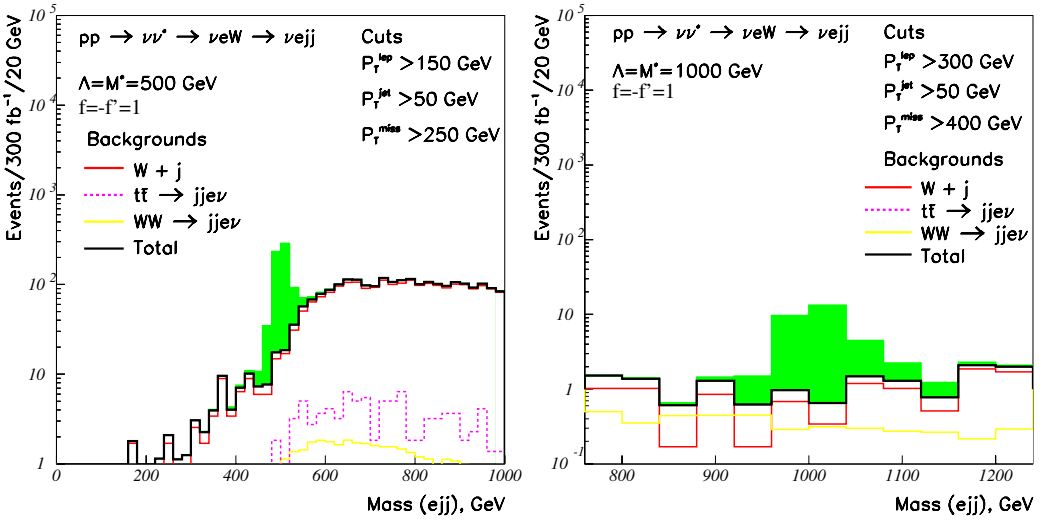

Fig. 5. Invariant mass distributions of $\nu^\star$ ($\to We$) and W's decay to jets for $m^\star = 500$ GeV (left) and $m^\star = 1000$ GeV (right). The integrated luminosity is 300 fb^{-1}. Shaded area represents the signal

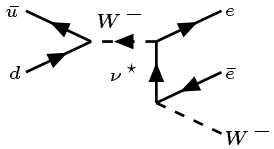

Fig. 6. Diagram for the production of an excited neutrino ($\nu^\star$) in association with an electron, where the $\nu^\star$ decays to W and positron

– The events were vetoed if the reconstructed invariant mass of any of two electrons was in the (80-100) GeV window. This Z production veto suppresses $W + Z$ background.
– The ratio $\sqrt{\not{P}_T}/[(P^x_{e1}+P^x_{e2})^2+(P^y_{e1}+P^y_{e2})^2]^{1/2}$, was required to be less than 0.25 to reduce the combinatorial background due to an extra electron in the event.
The last cut reflects the dynamics of excited neutrinos decay to an electron and a W and the subsequent decay of the W to an electron and a neutrino. An excited neutrino and the associated electron tend to be produced back-to-back. Therefore the associated electron and the excited neutrino decay products (the W-boson and the electron) are preferably lie in the same plane, which we denote here as the interaction plane (IP). Since a W-boson has a big boost (due to $m_{\nu^\star} \gg m_W$), the neutrino and the electron from a W-boson tend to be emitted along its direction, and therefore, again, prefer to lie in the IP. So, the projection of missing transverse momentum on the IP would be small for signal events.

The resulting transverse mass distributions (all combinations passing the cuts) for the excited neutrino masses 500, 1000, 1500, 2000, 2500 GeV are presented in Fig. 7(left) for the system of two electrons and the missing transverse momentum. One should note that the z-components of electron momentum were included in the definition of the transverse mass, presented in this figure. Signal distributions obtained with the cuts applied to each mass are superimposed on this figure.

In order to remove long tails of corresponding mass distributions in Fig. 7, which appeared as a result of the above superposition and obscured the visibility of adjacent mass peaks, the following additional cut was used for that purpose: the upper limit on the reconstructed mass of two electrons which were used to obtain the transverse mass of the excited neutrino had to be less than corresponding excited neutrino mass $M_{ee} < 500$ (1000, 1500) GeV for excited neutrino masses of 500 (1000, 1500) GeV, respectively.

W decays to $\mu\nu$. The corresponding signal signature consists of an electron, a muon and a neutrino, with accompanying second electron. This final state has less combinatorial background than the one considered above. The following cuts were used to separate the signal from background:

– The transverse momentum of each of the two electrons and of the muon was required to be at least 50 GeV and to be within the pseudorapidity acceptance of $\eta < 2.5$.
– The invariant mass of two electrons was required to be outside the (80-100) GeV mass window, in order to suppress $W + Z$ background.
– For better visibility of adjacent mass peaks, as in the case of $W \to e\nu$ decay channel, following additional cut was used: the upper limit on the reconstructed mass of the electron, which was used to obtain the invariant mass of the excited neutrino, and the muon had to be less than corresponding excited neutrino mass ($M_{ee} <$ 500 (1000, 1500) GeV for excited neutrino masses of 500 (1000, 1500) GeV, respectively.

To obtain the energy of the neutrino from W decay, the longitudinal component of neutrino momentum can be estimated from $\not{P}_T$ and muon momentum using only a

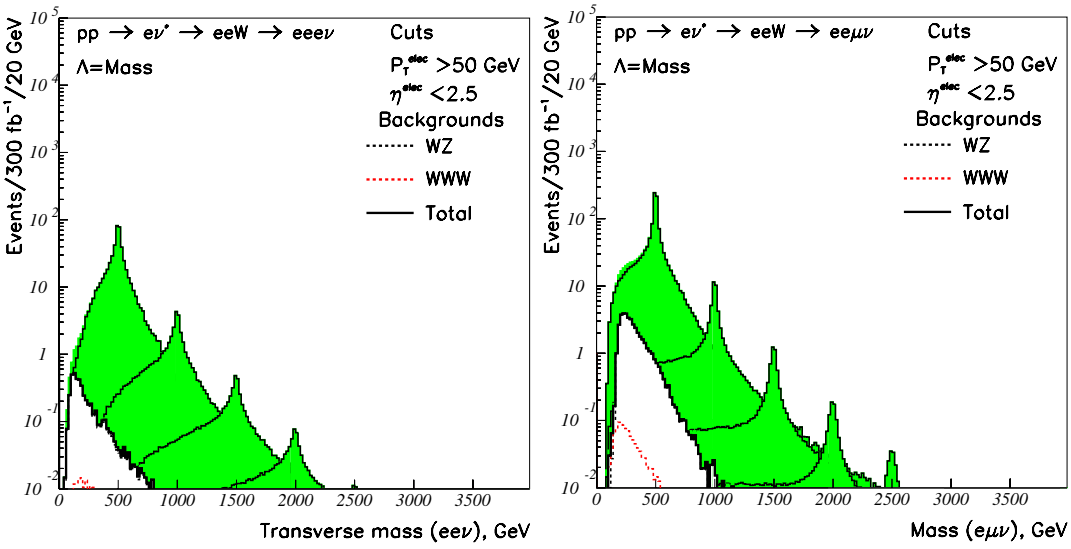

Fig. 7. Transverse mass distribution for $\nu^\star$ ($\to We$) with W decay to $e\nu$ (left) and invariant mass distribution for $\nu^\star$ ($\to We$) with W decay to $\mu\nu$ (right) for several signal masses superimposed. The integrated luminosity is 300 fb^{-1}

constraint on the W mass. The W mass value, $M_W = 80$ GeV, has been used to solve the quadratic equation and a pair of solutions for p_z^ν was obtained. The minimum between the two absolute values of p_z^ν has been taken to compute the invariant mass of the excited neutrino.

The resulting invariant mass distribution for the excited neutrino masses 500, 1000, 1500, 2000, 2500 GeV are presented in Fig. 7(right) for the system of electron-muon-neutrino. Signal distributions obtained with the cuts applied to each mass are superimposed on this figure. The distributions are normalized to an integrated luminosity of $L = 300$ fb^{-1}.

W decays to jets. In this case the final state consists of two electrons and two jets. For this reaction, the signal signature consists of an electron and two accompanying jets.

For this final state we considered the following SM background reactions as relevant:

- Z+jets production, where Z decays to an electron - positron pair.
- $W + Z$ production, where Z decays to an electron - positron pair and W to jets.
- WWW production, where two W's decay into an electron-neutrino pair and the third W into jets.

Background Z+jets were produced with PYTHIA and CTEQ5L for partonic transverse momentum $\hat{p}_T > 200$ GeV with corresponding cross section, $\sigma \times BR = 63$ pb.

For this signal signature, the following cuts were chosen:

- The transverse momentum of each of the two electrons was required to be at least 150 GeV and to be within the pseudorapidity region of $\eta < 2.5$.
- The transverse momenta of two jets were required to be at least 20 GeV.
- It was required to have the mass of $W \to$ jets reconstructed in the $(70 - 90)$ GeV mass window.
- The reconstructed invariant mass of two electrons was required to exceed 120 GeV in order to suppress Z+jets and $Z + W$ backgrounds with $Z \to ee$.

One notes that if W is very energetic (which could be the case for very large masses of excited neutrinos), the two jets may look like a single jet. Thus, these events would be lost in the analysis. We have estimated this effect and found that, for $m^\star$=1000 GeV, we may loose $\sim 9\%$ of signal events and up to $\sim 45\%$ events at $m^\star$=1500 GeV. But if we try to add events with the (1 jet + 2 electrons) topology, the number of background events rises substantially. Therefore, we do not use this signature in our analysis.

The resulting invariant mass distributions for the system of electron-jet-jet and the excited neutrino masses 500, 750, 1000, 1250 GeV are shown in Fig. 8. Signal distributions obtained with the cuts applied to each mass are superimposed on this figure. The distributions are normalized to an integrated luminosity of $L = 300$ fb^{-1}.

The presence of an extra electron in signal events leads to a combinatorial background which produces long tails in the mass distributions. Since the same selection cuts for different excited neutrino mass values have been used for this $\nu^\star$ decay channel, an additional mass window cut, which was in the order of $\pm 2\sigma$ width of the corresponding invariant mass signal distribution, was applied to determine the significance of the signal.

3.2.2 Channel with $\nu^\star \to Z\nu$ decay.

The decay of the excited neutrino to $Z\nu$, mediated by gauge interactions, is considered in this section. The corresponding diagram is presented in Fig. 9.

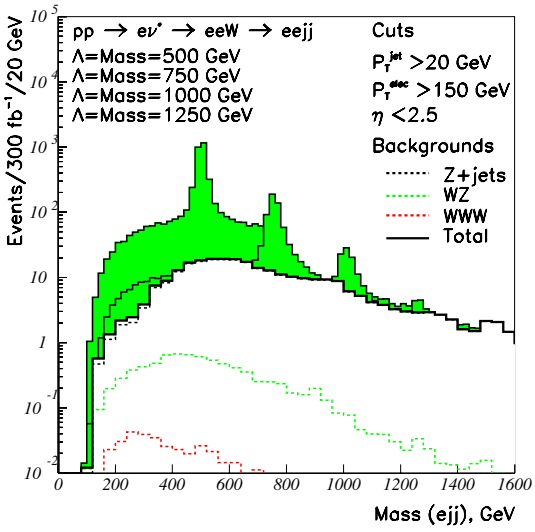

Fig. 8. Invariant mass distribution for $\nu^\star$ ($\rightarrow We$) with W decay mode to jets for several signal masses superimposed. The integrated luminosity is 300 fb^{-1}

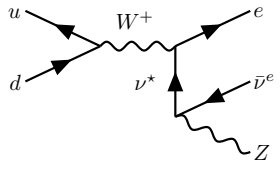

Fig. 9. Production and decay of the excited neutrino ($\nu^\star$) to Z and ν

For the Z decay, we studied the cases where Z decays to jets or Z decays into $\mu^+\mu^-$ pairs, to avoid the combinatorial background of $Z \rightarrow e^+e^-$ with the accompanying third electron.

In the case where Z decays to jets, the final state consists of an electron, a neutrino and two jets. The signal sought for is an energetic electron with two accompanying jets in the presence of a large missing transverse energy.

For this signal we considered three SM background:

- $W+$ jets production, where W decays to an electron and a neutrino.
- $t\bar{t}$ pair production, where one W decays to jets and the second W into an electron and a neutrino.
- WW pair production with the same decays as above.

Background $W+$jets were produced with PYTHIA and CTEQ5L for partonic transverse momentum $\hat{p}_T > 200$ GeV with the corresponding cross section, $\sigma \times BR = 17$ pb.

The following cuts were used to separate the signal from backgrounds:

- An electron was required, with transverse momentum to be at least 170 (200, 400) GeV for excited neutrino masses of 500 (750, 1000) GeV and to be emitted within the pseudorapidity acceptance of $\eta < 2.5$.
- The transverse momenta of two jets were required to be at least 40 GeV.
- The invariant mass of any two jet in the events was required to be consistent with the Z, in the $(80-100)$ GeV mass window, in order to suppress the dominant $W+$jets background.
- The missing transverse momentum, $\not{P}_T$, was required to be at least 400 GeV.

The resulting transverse mass distributions of the neutrino-jet-jet system are presented in Fig. 10 for the excited neutrino mass $m^\star = 500$ GeV (left). The distribution was normalized to an integrated luminosity of $L = 300$ fb^{-1}.

For the case where Z decays into $\mu^+\mu^-$ pairs, the final state consists of two muons, an electron and a neutrino. The signal signature for this subprocess is two muons accompanied by an energetic electron and missing transverse energy.

The natural SM background for this subprocess is $W+Z$ production, where W decays to $e\nu$ and Z decays into muons.

The following cuts were used to separate the signal from the backgrounds:

- The transverse momentum of an electron was required to be at least 120 GeV and to be emitted within the pseudorapidity acceptance of $\eta < 2.5$.
- The transverse momenta of two muons were required to be at least 10 GeV.
- The invariant mass of two muons was required to be consistent with the Z in the (80-100) mass window.
- Events with the $e + \nu$ mass reconstructed in the $(70-90)$ GeV mass window were vetoed to suppress background from W's.
- The missing transverse momentum was required to be at least 100 GeV.

The resulting transverse mass distribution of two muons combined with missing transverse energy is presented in Fig. 10 (right) for $m^\star = 500$ GeV and an integrated luminosity of $L = 300$ fb^{-1}.

There is a possibility to consider the case where Z decays into e^+e^- pairs, which gives three electrons and a neutrino in the final state. However, requiring the condition on the invariant mass of two electrons to be in the (80-100) GeV region, we lose signal events due to combinatorics. Even imposing rather loose cuts for 3 electrons (e.g., transverse momenta larger than 50 GeV), the number of signal events in this decay channel is ~ 10 times less than for the case where $Z \rightarrow \mu^+\mu^-$.

3.2.3 Channel with $\nu^\star \rightarrow \nu\gamma$ decay.

Another interesting subprocess is the decay of an excited neutrino to ν and a photon (Fig. 11).

The signal consists of a photon and a neutrino in the presence of an energetic electron. The natural SM background for this subprocess is $W+\gamma$ production where the W decays to e and ν.

The cuts used to separate the signal from background are:

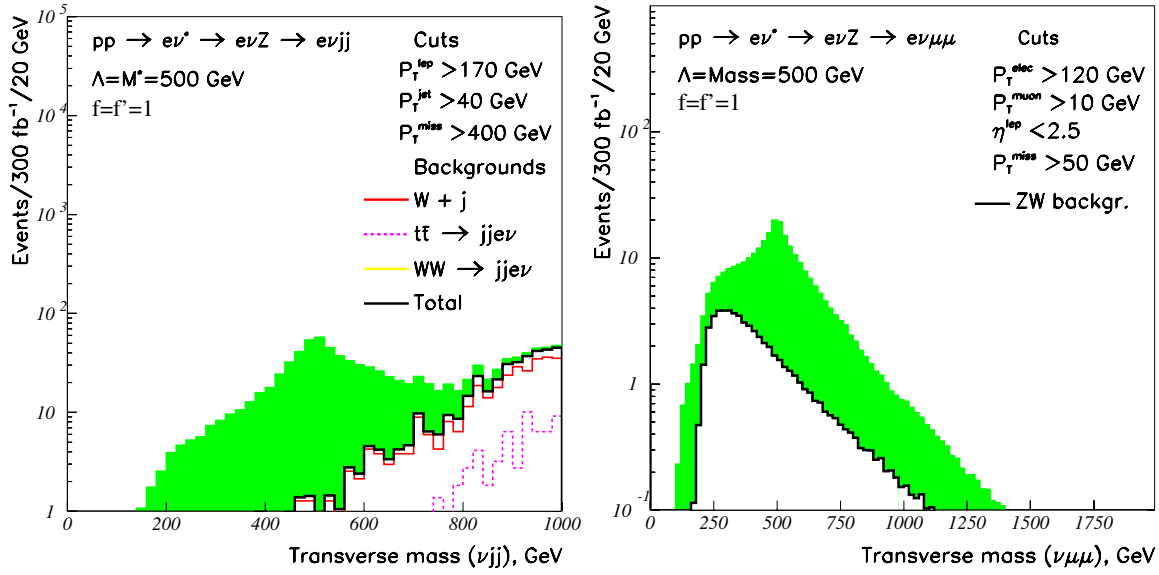

Fig. 10. Transverse mass distributions of $\nu^\star$ ($\to Z\nu$) for Z $\to$ 2 jets (left) and $\nu^\star$ ($\to Z\nu$) for Z decay mode to $\mu^+\mu^-$ (right) for $m^\star = 500$ GeV. The integrated luminosity is 300 fb^{-1}. Shaded area represents the signal

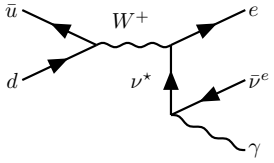

Fig. 11. Diagram for the production of an excited neutrino ($\nu^\star$) in association with an electron, where $\nu^\star$ decays to a photon and neutrino

– The transverse momenta of an electron and a photon were required to be at least 50 GeV, and to be within the pseudorapidity acceptance of $\eta < 2.5$.

The resulting transverse mass distribution of the electron and missing transverse momentum is presented in Fig. 12 for several signal masses superimposed and an integrated luminosity of $L = 300$ fb^{-1}.

4 Mass reach

In Table 3, the corresponding signal significances, for all studied subprocesses, are presented for an integrated luminosity of $L = 300$ fb^{-1}. The number of accepted signal and background events (including, when applicable, combinatorial background) were defined in the selected mass bin width (ΔM). The width of the mass bin was taken to be $\pm 2\sigma$, where σ is the rms around the peak of the invariant mass distribution for the excited neutrino. The signal significance was calculated in the following way: first, we evaluated the probability of the presence of the signal assuming a Poisson distribution of the errors and then we translated this probability into number of standard deviations for a Gaussian distribution.

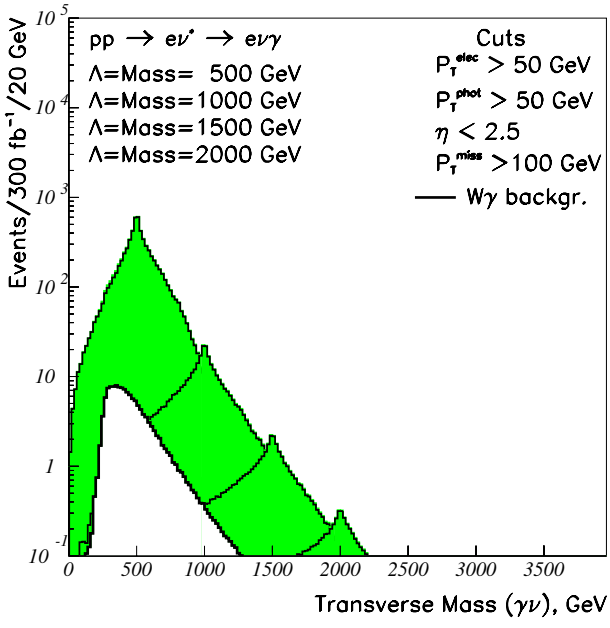

Fig. 12. Transverse mass distribution of $\nu^\star \to \nu\gamma$ for several signal masses superimposed. The integrated luminosity is 300 fb^{-1}

As can be seen from Table 3, the highest reach for excited neutrino production would be available in decays of the excited neutrino to ν and a photon (due to a low background level) for a non-zero $\nu\nu^\star\gamma$ coupling of $f = -f' = 1$. However, the excited neutrino decay channel involving W is also promising. In the case of $f = f' = 1$, the $\nu\nu^\star\gamma$ coupling vanishes and excited neutrino decay channel involving W becomes clearly dominant. The mass reach in the $(eee\nu)$ and $(ee\mu\nu)$ decay channels is is around

Table 3. The signal significances, $Signif(\sigma)$. S stands for a signal, B for the total background. Number of events are calculated for an integrated luminosity of $L = 300$ fb^{-1}. The results assume $\Lambda = m^\star$ and are given for various couplings within selected mass bin width (ΔM)

$m^\star(GeV) \to$	500	750	1000	1250	1500
$q\bar{q} \to \nu\nu^\star \to \nu eW \to \nu ejj$					
ΔM, GeV	28	72	92	116	–
S	555	90	24	5.5	–
B	129	7	3.3	1.2	–
$Signif(\sigma)$	49	34	7.0	3.0	–
$q\bar{q} \to e\nu^\star \to eeW \to eee\nu + ee\mu\nu$					
ΔM, GeV	32	98	100	102	132
S	1405	354	64	30	9
B	11	3	0.3	0.1	0.02
$Signif(\sigma)$	423	204	117	95	6.4
$q\bar{q} \to e\nu^\star \to eeW \to eejj$					
ΔM, GeV	36	92	120	160	180
S	2608	508	97	17	4.6
B	86	64	47	5.3	4.7
$Signif(\sigma)$	281	64	10	5	1.7
$q\bar{q} \to e\nu^\star \to e\nu Z \to e\nu\mu\mu$, $f = f' = 1$					
ΔM, GeV	100	260	400	–	–
S	123	20	4	–	–
B	21	8.3	1.7	–	–
$Signif(\sigma)$	27	5.0	2.2	–	–
$q\bar{q} \to e\nu^\star \to e\nu Z \to e\nu jj$, $f = f' = 1$					
ΔM, GeV	160	240	320	400	-
S	419	97	21	5	-
B	24	19	4	2	-
$Signif(\sigma)$	86	22	6	2.7	-
$q\bar{q} \to e\nu^\star \to \gamma e\nu$, $f = -f' = 1$					
ΔM, GeV	120	160	200	204	240
S	3755	533	151	45	18
B	62	11	3.7	1.2	0.5
$Signif(\sigma)$	477	161	78	41	7.4

1800 GeV, and very similar for the choice of couplings $f = f' = 1$ or $f = -f' = 1$. At lower values of excited neutrino masses, the signature with $(eejj)$ in the final state is more promising due to a better statistical significance.

Excited neutrino decay channels involving Z bosons, due to the smaller branching ratio, can be used only to confirm excited neutrino observations, obtained from other channels. This channel could be observable for $f = f' = 1$ with $m_{\nu^\star}$ only below 1 TeV. The case $f = -f' = 1$ is even less promising and, therefore, is not presented in Table 3 — the number of signal events decreases by a factor of 3.5 according to the $\nu^\star \to Z\nu$ branching ratio (see Table 2).

The results of the present study can be also summarized in the $(m_{\nu^\star} - \Lambda)$ LHC reach plot, which is presented in Fig. 13. Both cases: $f = f' = 1$ and $f = -f' = 1$ have a very similar reach. This plot presents the combined results for $\nu\gamma$ and We channels of the excited neutrinos decay. The parameter space below black(magenta) curves is excluded at $\sigma = 3(5)$ level of the statistical significance. One can see, for example, that for $\Lambda \sim m_{\nu^\star} \lesssim 2.1$ TeV can be excluded at 3σ level while $\Lambda \sim m_{\nu^\star} \lesssim 1.8$ TeV can be discovered at the LHC at 5σ level.

5 Conclusions

We have studied the potential of the CERN LHC to observe excited neutrinos production within the framework of a composite model of quarks and leptons.

Analysis of reconstructed invariant mass distributions of the excited neutrinos singly produced at the LHC, shows that, clean $e\nu\gamma$, $eee\nu$, $ee\mu\nu$ and $eejj$ signatures are expected to be found. We have studied two possible

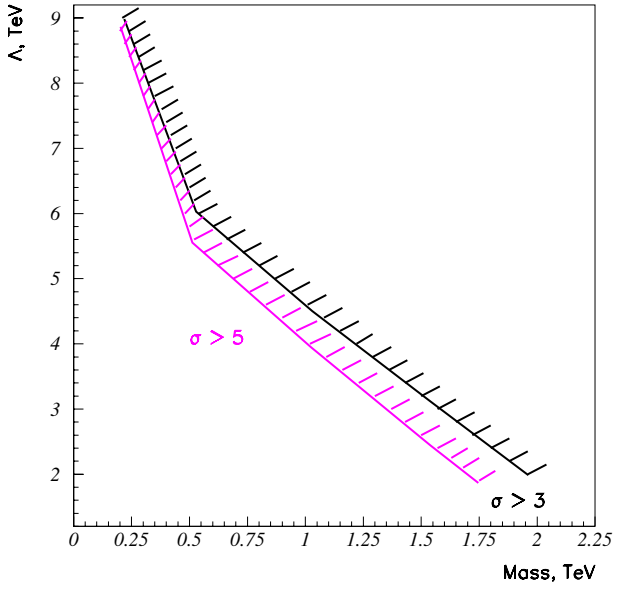

Fig. 13. The reach of Λ as a function of the $m_{\nu^\star}$. The integrated luminosity is 300 fb^{-1}

choices of coupling parameters: the case of $f = -f' = 1$, which gives rise to a non-vanishing $\nu\nu^\star\gamma$ coupling, and the case of $f = f' = 1$. For $f = -f' = 1$, the highest reach is expected for the $e\nu\gamma$ final state, while in the case of $f = f' = 1$, $eee\nu$, $ee\mu\nu$, and $eejj$ final states look most promising to reach the sensitivity for large excited neutrino masses. Our results are summarized in Table 3 and Fig. 13. The latter presents the LHC reach in the $(m_{\nu^\star} - \Lambda)$ plane for excited neutrino production. We have found that singly produced excited neutrinos could be accessible up to a mass of 1.8 TeV at LHC for $\Lambda \sim m_{\nu^\star}$ case, assuming an integrated luminosity of $L = 300$ fb^{-1}.

Acknowledgements. This work has been performed within the ATLAS Collaboration with the help of the simulation framework and tools which are the result of the collaboration-wide efforts. We would like also to thank G. Azuelos, H. Baer, O. Çakır, D. Froidevaux, F. Gianotti, I. Hinchliffe, L. Poggioli, L. Reina for their comments about the subject. C.L. and R.M. thank NSERC/Canada for their support. This research was partially supported by the U.S. Department of Energy under contracts number DE-FG02-97ER41022 and DE-FG03-94ER40833.

References

1. H. Terazawa, M. Yasue, K. Akama, M. Hayashi. Phys. Lett. B **112**, 387 (1982): F.M. Renard. Il Nuovo Cimento, **77**A, 1 (1983); A. De Rujula, L. Maiani, R. Petronzio: Phys.Lett. B **140**, 253 (1984); E.J. Eichten, K.D. Lane, M.E. Peskin. Phys.Rev. D **50**, 811 (1983)
2. H. Terazawa, Y. Chikashige, K. Akama, Phys.Rev. D **15**, 480 (1977); J-J. Dugne, S. Fredriksson, J. Hansson, Europhys. Lett. **57**, 188 (2002) [arXiv:hep-ph/0208135]
3. Y. Ne'eman. Phys.Lett. B **82**, 69 (1979)
4. U. Baur, M. Spira, P.M. Zerwas. Phys. Rev. D **42**, 815 (1990)
5. ATLAS Detector and Physics Performance Technical Design Report. CERN/LHCC/99-14/15 (1999)
6. P. Achard et al., [L3 Collaboration], Phys. Lett. B **568**, 23 (2003) [arXiv,hep-ex/0306016]; S. Andringa et al., [DELPHI Collaboration], CERN-OPEN-99-469 Prepared for 34th Rencontres de Moriond, Electroweak Interactions and Unified Theories, Les Arcs, France, 13–20 Mar 1999; B. Vachon, Nucl.Phys. Proc. Suppl. **98**, 148 (2001); R.Barate et al., [ALEPH Collaboration], Eur. Phys. J. C **12**, 183 (2000) [arXiv,hep-ex/9904011]
7. L. Bellagamba [H1 and ZEUS Collaborations], Prepared for 31st International Conference on High Energy Physics (ICHEP 2002), Amsterdam, The Netherlands, 24–31 Jul 2002; U.F. Katz [H1 Collaboration], arXiv, hep-ex/0212049; C. Adloff et al., [H1 Collaboration], Phys.Lett. B **548**, 35 [arXiv,hep-ex/0207038] (2002); A. Weber, Acta Phys. Polon. B **33**, 3899 (2002) [arXiv,hep-ex/0207032]; C. Adloff et al., [H1 Collaboration], Phys. Lett. B **479**, 358 (2000) [arXiv,hep-ex/0003002]
8. E. Boos, A. Vologdin, D. Toback and J. Gaspard, Phys. Rev. D **66**, 013011 [arXiv,hep-ph/0111034] (2002); J.A. Green [D0 Collaboration], arXiv, hep-ex/0004035; B. Abbott et al., [D0 Collaboration], Phys. Rev. Lett. **82**, 4769 [arXiv,hep-ex/9812010] (1999); A. Bodek [CDF Collaboration], Nucl. Phys. Proc. Suppl. **66**, 96 (1998); E. Gallas [D0 Collaboration], FERMILAB-CONF-97-390-E, Prepared for International Europhysics Conference on High-Energy Physics (HEP 97), Jerusalem, Israel, 19–26 Aug 1997; P. deBarbaro, A. Bodek, B.J. Kim, Q. Fan, R. Harris [CDF Collaboration], FERMILAB-CONF-96-356, Proc. of 1996 DPF / DPB Summer Study on New Directions for High-energy Physics (Snowmass 96), Snowmass, CO, 25 Jun – 12 Jul 1996
9. U. Baur, I. Hinchliffe, D. Zeppenfeld, Int. J. Mod. Phys. A **2**, 1285 (1987)
10. O. Çakır, R. Mehdiyev, Phys. Rev. D **60**, 034004 (1999); O. Çakır, C. Leroy, R. Mehdiyev, Phys. Rev. D **62**, 114018 (2000); O. Çakır, C. Leroy, R. Mehdiyev, Phys. Rev. D **63**, 094014 (2001)
11. O.J.P. Eboli, S.M. Lietti, P. Mathews, Phys. Rev. D **65**, 075003 (2002) [arXiv,hep-ph/0111001]
12. O. Çakır, C. Leroy, R. Mehdiyev, A. Belyaev, Eur. Phys. J. Direct C **30**, 005 (2003) [arXiv,hep-ph/0212006]
13. J.H. Kuhn, P.M. Zerwas, Phys. Lett. B **147**, 189 (1984); J.H. Kuhn, H.D. Thoel, P.M. Zerwas, Phys.Lett. B **158**, 270 (1985)
14. F.M. Renard, Phys. Lett. B **116**, 264 (1982)
15. N. Cabibbo, L. Maiani, Y. Strivastava, Phys. Lett. B **139**, 459 (1984); F.M. Renard, Phys. Lett. B **126**, 59 (1983); B **139**, 449 (1984); K. Hagiwara, S. Komamiya, D. Zeppenfeld, Z. Phys. C **29**, 115 (1985)
16. H.L. Lai et al., CTEQ Coll., Phys. Rev. D **51**, 4763 (1995)
17. A. Pukhov at al., arXiv,hep-ph/9908288 (1999)
18. A.S. Belyaev et al., arXiv, hep-ph/0101232 (2001)
19. T. Sjostrand, Computer Phys. Communications **82**, 74 (1994)
20. E. Richter-Was, D. Froidevaux, L. Poggioli, ATLAS Note PHYS-98-131 (1998)
21. ATLAS Collaboration, Technical Proposal, Report No. CERN/LHCC/94-43 (1994)